

Characterization of the Terminal Iron(IV) Imides  $\{[\text{PhBP}^{\text{tBu}}_2(\text{pz}')] \text{Fe}^{\text{IV}} \equiv \text{NAd}\}^+$ 

Christine M. Thomas, Neal P. Mankad, and Jonas C. Peters\*

Division of Chemistry and Chemical Engineering, Arnold and Mabel Beckman Laboratories of Chemical Synthesis, California Institute of Technology, Pasadena, California 91125

Received January 27, 2006; E-mail: jpeters@caltech.edu

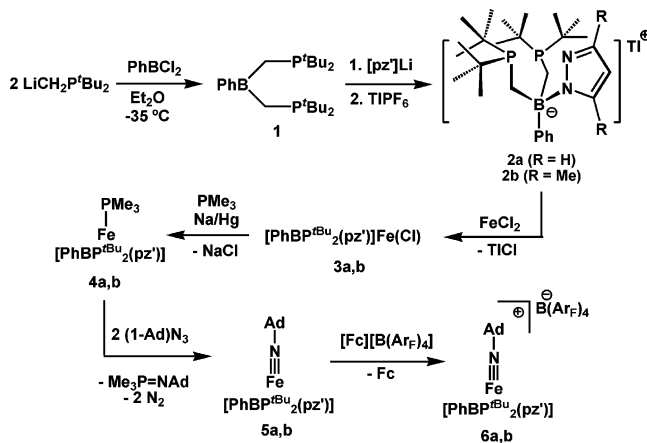
Although implicated as intermediates in group transfer reactions,<sup>1</sup> mid-to-late first row transition metals (e.g., Mn, Fe, Co, Ni) featuring terminal imido/nitrene functionalities are rare.<sup>2</sup> To date, the only examples of structurally characterized mononuclear iron imides are those supported by tris(phosphino)borate ligands.<sup>3</sup> These species have been reported in the Fe(III) and Fe(II) oxidation states. In the Fe(III) state, they have been accessed via oxidative nitrene transfer from organic azides using low valent Fe<sup>I</sup> precursors. The  $[\text{PhBP}^{\text{R}}_3]\text{Fe}^{\text{III}}(\text{NR})$  complexes that have been isolated all show electrochemically reversible Fe<sup>III/II</sup> couples, and chemical reduction typically provides their corresponding d<sup>6</sup>  $\{[\text{PhBP}^{\text{R}}_3]\text{Fe}^{\text{II}}(\text{NR})\}^-$  analogues in high yield. Well-defined Fe<sup>IV</sup>=NR species have proven generally more elusive,<sup>4</sup> though thoroughly characterized examples of Fe<sup>IV</sup>=O species are now well-known.<sup>5</sup> To the best of our knowledge, the single report of a complex that can be formulated as an Fe(IV) imide concerns Lee's tetranuclear cluster  $\text{Fe}_4(\mu_3\text{-N}^t\text{-Bu})_4(\text{N}^t\text{-Bu})\text{Cl}_3$ , isolated in only 1–2% yield.<sup>6</sup> Mössbauer data for this species were consistent with a cluster featuring three Fe(III) centers and one Fe(IV) center. Herein we describe a new hybrid pyrazolyl/phosphinoborate ligand that can support pseudotetrahedral iron in the +1, +2, +3, and +4 oxidation states. The +3 and +4 oxidation states are stabilized by the terminal Fe≡NR imide linkage.

Access to the required bis(phosphino)pyrazolylborate<sup>7</sup> ligand is achieved by initial preparation of the bis(phosphino)borane precursor  $\text{PhB}(\text{CH}_2\text{P}^{\text{tBu}}_2)_2$  (**1**) via metathesis between  $\text{PhBCl}_2$  and 2 equiv of  $\text{LiCH}_2\text{P}^{\text{tBu}}_2$  (Scheme 1). Reaction of  $[\text{pz}]\text{Li}$  with **1** (pz = pyrazolyl), followed immediately by salt metathesis with TlPF<sub>6</sub>, leads to the clean formation of solid white  $[\text{PhBP}^{\text{tBu}}_2(\text{pz})]\text{Tl}$  (**2a**) in 66% isolated yield.<sup>8</sup> The use of the bulky  $\text{LiCH}_2\text{P}^{\text{tBu}}_2$  carbanion is critically important in the preparation of this type of hybrid borate ligand because (i) effective di- rather than trisubstitution at boron can be achieved, which could not be realized using less hindered carbanions, such as  $\text{LiCH}_2\text{P}^{\text{R}}_2$  and  $\text{LiCH}_2\text{PPh}_2$ ; (ii) the borane product,  $\text{PhB}(\text{CH}_2\text{P}^{\text{tBu}}_2)_2$  (**1**), does not appear to dimerize to an appreciable degree in solution. This fact allows the efficient introduction of a third donor arm.

Metathesis of **2a** with  $\text{FeCl}_2$  leads to the clean formation of the high spin ( $S = 2$ ) complex  $[\text{PhBP}^{\text{tBu}}_2(\text{pz})]\text{FeCl}$  (**3a**), isolated in 69% yield as a yellow crystalline solid. Solution <sup>1</sup>H NMR data for **3a** are suggestive of a monomeric structure in solution, in accord with the calculated solution Evans' method magnetic moment at 295 K ( $5.2 \mu_{\text{B}}$ ).<sup>9</sup> However, the 100 K X-ray crystal structure of **3a** establishes a dimeric structure with bridging chlorides and a crystallographic center of symmetry in the solid state.

Following an overall methodology that proved effective for the synthesis of Fe(III) imides previously,<sup>3</sup> one-electron reduction of **3a** with sodium/mercury amalgam in the presence of excess  $\text{PMe}_3$  generates the high spin d<sup>7</sup> precursor  $[\text{PhBP}^{\text{tBu}}_2(\text{pz})]\text{Fe}(\text{PMe}_3)$  (**4a**) as a pale green crystalline solid (65% isolated yield;  $\mu_{\text{eff}} = 4.2 \mu_{\text{B}}$ ). The reaction between **4a** and 2 equiv of 1-adamantyl azide (1-AdN<sub>3</sub>) generates the expected Fe(III) imide  $[\text{PhBP}^{\text{tBu}}_2(\text{pz})]\text{Fe} \equiv \text{NAd}$  (**5a**) as a red-brown low spin species ( $2.0 \mu_{\text{B}}$  in  $\text{C}_6\text{D}_6$ ), in addition

Scheme 1



to a stoichiometric equivalent of (1-Ad)N=PMe<sub>3</sub>. The EPR spectrum of **5a** displays a rhombic signal that was simulated (see SI) to provide the  $g$  values  $g_1 = 2.96$ ,  $g_2 = 1.95$ , and  $g_3 = 1.88$  (Figure 1A), a spectrum similar to those of related  $[\text{PhBP}^{\text{R}}_3]\text{Fe}^{\text{III}} \equiv \text{NR}$  imides.<sup>3</sup>

The cyclic voltammetry of **5a** reveals very different features from those observed for  $[\text{PhBP}^{\text{R}}_3]\text{Fe}^{\text{III}}(\text{NR})$  imides (Figure 1B). For example, the cyclic voltammogram of previously reported  $[\text{PhBP}^{\text{tBu}}_3]\text{Fe} \equiv \text{NAd}$ <sup>3b</sup> features a fully reversible reductive wave at  $-1.79$  V and an irreversible oxidative wave at ca.  $-0.45$  V. This latter process presumably reflects a one-electron oxidation to an unstable Fe(IV) species. By contrast, complex **5a** exhibits a completely irreversible reductive wave at  $-2.20$  V, indicating that the Fe(II) imide anion is, in this case, unstable. The oxidative irreversible wave at  $-1.26$  V appears only after scanning through the  $-2.20$  V wave, indicating that it represents a byproduct of the one-electron reduction of **5a**. More interesting, however, is the presence of a quasi-reversible feature at  $-0.72$  V for **5a** (at 100 mV/s; 22 °C). This wave becomes fully reversible at ambient temperature when the scan rate is increased to 500 mV/s. It represents an Fe<sup>IV/III</sup> redox couple and suggests that “ $\{[\text{PhBP}^{\text{tBu}}_2(\text{pz})]\text{Fe}^{\text{IV}} \equiv \text{NAd}\}^+$ ” might be modestly stable.

In accord with these electrochemical data, **5a** can be chemically oxidized with  $[\text{Fc}][\text{B}(\text{Ar}_\text{F})_4]$  ( $\text{Ar}_\text{F} = 3,5\text{-(CF}_3)_2\text{-C}_6\text{H}_3$ ) at low temperature ( $-50$  °C) in THF solution to generate a green, cationic species formulated as  $\{[\text{PhBP}^{\text{tBu}}_2(\text{pz})]\text{Fe}^{\text{IV}} \equiv \text{NAd}\}^+[\text{B}(\text{Ar}_\text{F})_4]^-$  (**6a**). A single set of paramagnetic resonances is observed for **6a** in its <sup>1</sup>H NMR spectrum at  $-50$  °C (see SI), distinct from the resonances observed for **5a**. Using an optical dip-probe assembly, the appearance of absorption bands at 580 and 677 nm are readily observed at low temperature upon addition of the ferrocenium oxidant (see SI). We also established that the addition of 1 equiv of  $\text{CoCp}_2$  to **6a** generated in situ in THF-*d*<sub>8</sub> solution regenerated **5a** cleanly. The half-life of **6a** is approximately 50 min at  $-40$  °C in THF-*d*<sub>8</sub>, and it must therefore be manipulated at temperatures below  $-40$  °C. Solution magnetic data collected at low temperature ( $\mu_{\text{eff}} = 3.1(2) \mu_{\text{B}}$  in THF-*d*<sub>8</sub>, 222 K; avg of 4 runs) indicate two unpaired

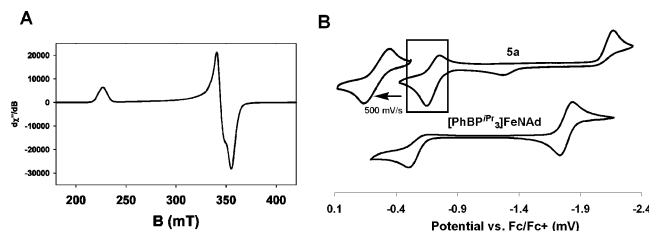


**Figure 1.** (A) EPR spectrum of **5a** with  $g_1 = 2.96$ ,  $g_2 = 1.95$ , and  $g_3 = 1.88$  (in 2-methyltetrahydrofuran glass at 20 K, 9.474 GHz). (B) Cyclic voltammetry of **5a** (0.40 M [ $^n\text{Bu}_4\text{N}$ ][ $\text{ClO}_4$ ] in THF, scan rate = 100 mV/s (full), 500 mV/s (inset) and [ $\text{PhBP}^{\text{Bu}_2}$ ] $\text{Fe}\equiv\text{NAd}$  (0.40 M [ $^n\text{Bu}_4\text{N}$ ][ $\text{PF}_6$ ] in THF).

electrons ( $S = 1$ ), consistent with the ground state electronic configuration  $(d_{z^2})^2(d_{xy})^1(d_{x^2-y^2})^1(d_{xz})^0(d_{yz})^0$ .

We undertook a crystallographic investigation of **5a** and **6a** to confirm their connectivities and to examine their Fe–N bond distances and Fe–N<sub>imide</sub>–C bond angles for comparison with [ $\text{PhBP}^{\text{R}_3}$ ] $\text{Fe}\equiv\text{NR}$  imides. For the case of **5a**, the crystals that we obtained were twinned, regardless of the method employed for crystallization. Its structure could nonetheless be refined isotropically to confirm its pseudotetrahedral geometry (see SI). Evident from its isotropic structure is an expectedly short Fe–N<sub>imide</sub> bond distance (1.63 Å) and a nearly linear C–N3–Fe angle ( $169^\circ$ ).<sup>3</sup>

Owing to the thermal instability of **6a**, its XRD analysis proved to be a more challenging experiment. Single green crystals could be obtained by storing a THF/petroleum ether solution at  $-78^\circ\text{C}$  for several days, and XRD analysis confirmed its proposed assignment (see SI). To obtain a better quality data set, we set out to prepare an analogue of **6a** of greater kinetic stability. We thus pursued a [ $\text{PhBP}^{\text{Bu}_2}(\text{pz}')$ ] $^-$  derivative substituted by methyl groups at the 3 and 5 positions. The required precursor ([ $\text{PhBP}^{\text{Bu}_2}(\text{pz}^{\text{Me}_2})$ ]- $\text{Ti}$ , **2b**) and an analogous series of iron complexes (**3b**–**6b**, Scheme 1) were readily prepared by the same procedures described above. The imide cation **6b** indeed exhibits far greater thermal stability than **6a**. Its cyclic voltammetry is very similar to that of **6a**, and the  $\text{Fe}^{\text{IV/III}}$  redox couple is reversible even at slower scan rates (e.g., 100 mV/s). **6b** can even be isolated in pure form at ambient temperature (86.7% yield) and manipulated without appreciable degradation for short periods. X-ray data sets were obtained for **5b** (disordered structure; see SI) and **6b**. The anisotropically refined X-ray crystal structure of {[ $\text{PhBP}^{\text{Bu}_2}(\text{pz}^{\text{Me}_2})$ ] $\text{Fe}^{\text{IV}}\equiv\text{NAd}$ }{[ $\text{B}(\text{Ar}_f)_4$ ]} **6b** is shown in Figure 2. The structure reveals the anticipated pseudotetrahedral iron cation and its tetra(aryl)borate counteranion. The Fe–N3 bond distance (1.634(4) Å) and the Fe–N<sub>imide</sub>–C bond angle ( $176.2(3)^\circ$ ) are similar to the parameters obtained for crystallographically characterized [ $\text{PhBP}_3$ ] $\text{Fe}$  imides in the +3 and +2 oxidation states.<sup>3</sup> Assuming that the two unpaired electrons of **6b** reside in relatively nonbonding d-orbitals, as predicted from simple MO considerations,<sup>2b,3c</sup> the Fe–N bond should retain its triple bond character (i.e.,  $\text{Fe}^{\text{IV}}\equiv\text{NR}^+$ ) and the Fe–N distance is therefore not expected to change to a large extent upon oxidation.

In summary, whereas iron imides had been previously obtained in the +3 and +2 oxidation states using [ $\text{PhBP}^{\text{R}_3}$ ] $\text{Fe}$  systems, we now find that imides in the +3 and +4 oxidation states are accessible using [ $\text{PhBP}^{\text{Bu}_2}(\text{pz}')$ ] $\text{Fe}$  systems. It is remarkable that terminally bonded  $\text{L}_3\text{Fe}\equiv\text{NR}$  species have now been characterized in three distinct oxidation states using phosphine–borate ligands given the paucity of such species more generally. The cause of the increased stability of the  $\text{Fe}^{\text{IV}}\equiv\text{NR}$  linkage in the [ $\text{PhBP}^{\text{Bu}_2}(\text{pz}')$ ] $\text{Fe}$  system described herein is an interesting issue and might in part be attributed to (i) a cathodic shift in the  $\text{Fe}^{\text{IV/III}}$  potential by comparison to previous [ $\text{PhBP}^{\text{R}_3}$ ] $\text{Fe}$  imide systems, which in turn might lend added stability to the ligand borate unit and/or (ii) to the lower

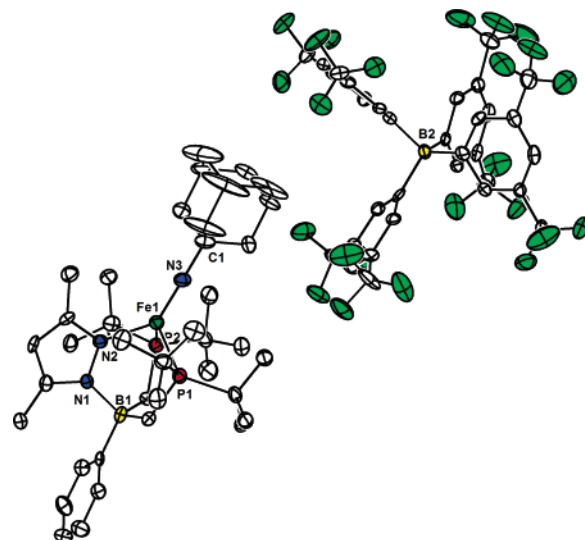


**Figure 2.** Anisotropically refined thermal ellipsoid representation of {[ $\text{PhBP}^{\text{Bu}_2}(\text{pz}^{\text{Me}_2})$ ] $\text{Fe}^{\text{IV}}\equiv\text{NAd}$ }{[ $\text{B}(\text{Ar}_f)_4$ ]} (**6b**); two molecules of THF and all hydrogen atoms have been omitted for clarity; Fe–N3 1.634(4) Å; Fe–N3–C1  $176.2(3)^\circ$ .

symmetry of the [ $\text{PhBP}^{\text{Bu}_2}(\text{pz}')$ ] ligand, and the compatibility of this lower symmetry with a  $d^4$  triplet electronic configuration.

**Acknowledgment.** We acknowledge Larry Henling for crystallographic assistance, and Dr. Mark Mehn for assistance with EPR spectroscopy. We thank the NIH for financial support (GM 070757), and N.P.M. is grateful for an NSF graduate fellowship.

**Supporting Information Available:** Detailed experimental procedures for **1**, **2a,b**–**6a,b**, all characterization data, and crystallographic details for **3a**, **5a**, **5b**, **6a**, and **6b**. This material is available free of charge via the Internet at <http://pubs.acs.org>.

## References

- (a) Li, Z.; Conser, K. R.; Jacobsen, E. N. *J. Am. Chem. Soc.* **1993**, *115*, 5326. (b) Evans, D. A.; Faul, M. M.; Bilodeau, M. T. *J. Am. Chem. Soc.* **1994**, *116*, 2742. (c) DuBois, J.; Tomooka, C. S.; Hong, J.; Carreira, E. M. *Acc. Chem. Res.* **1997**, *30*, 364. (d) Wigley, D. E. In *Progress in Inorganic Chemistry*; Karlin, K. D., Ed.; Wiley-Interscience: New York, 1994; Vol. 42, pp 239–482. (e) Eikey, R. A.; Abu-Omar, M. M. *Coord. Chem. Rev.* **2003**, *243*, 83.
- For recent examples, see: (a) Mindiola, D. J.; Hillhouse, G. L. *J. Am. Chem. Soc.* **2001**, *123*, 4623. (b) Jenkins, D. M.; Betley, T. A.; Peters, J. C. *J. Am. Chem. Soc.* **2002**, *124*, 5272. (c) Eikey, R. A.; Khan, S. I.; Abu-Omar, M. M. *Angew. Chem., Int. Ed.* **2002**, *41*, 3592. (d) Dai, X.; Kapoor, P.; Warren, T. H. *J. Am. Chem. Soc.* **2004**, *126*, 4798. (e) Hu, X.; Meyer, K. *J. Am. Chem. Soc.* **2004**, *126*, 16322.
- (a) Brown, S. D.; Betley, T. A.; Peters, J. C. *J. Am. Chem. Soc.* **2003**, *125*, 322. (b) Betley, T. A.; Peters, J. C. *J. Am. Chem. Soc.* **2003**, *125*, 10782. (c) Brown, S. D.; Peters, J. C. *J. Am. Chem. Soc.* **2004**, *126*, 4538. (d) Brown, S. D.; Peters, J. C. *J. Am. Chem. Soc.* **2005**, *127*, 1913.
- $\text{Fe}(\text{IV})$  imides have been implicated as intermediates in nitrene transfer reactions: (a) Lucas, R. L.; Powell, D. R.; Borovik, A. S. *J. Am. Chem. Soc.* **2005**, *127*, 11596. (b) Jensen, M. P.; Mehn, M. P.; Que, L., Jr. *Angew. Chem., Int. Ed.* **2003**, *42*, 4357.
- For recent non-heme iron examples, see: (a) Rohde, J.-U.; In, J.-H.; Lim, M. H.; Brennessel, W. W.; Bukowski, M. R.; Stubna, A.; Münck, E.; Nam, W.; Que, L., Jr. *Science* **2003**, *299*, 1037. (b) Klinker, E. J.; Kaiser, J.; Brennessel, W. W.; Woodrum, N. L.; Cramer, C. J.; Que, L., Jr. *Angew. Chem., Int. Ed.* **2005**, *44*, 3690. (c) Bukowski, M. R.; Koehn, K. D.; Stubna, A.; Bominaar, E. L.; Halfen, J. A.; Münck, E.; Nam, W.; Que, L., Jr. *Science* **2005**, *310*, 1000. (d) Grapperhaus, C. A.; Mienert, B.; Bill, E.; Weyhermüller, T.; Wieghardt, K. *Inorg. Chem.* **2000**, *39*, 5306.
- Verma, A. K.; Nazif, T. N.; Achim, C.; Lee, S. C. *J. Am. Chem. Soc.* **2000**, *122*, 11013.
- A related bis(pyrazole)(phosphine)borate ligand was reported recently: Casado, M. A.; Hack, V.; Camarero, J. A.; Ciriano, M. A.; Tejedor, C.; Oro, L. A. *Inorg. Chem.* **2005**, *44*, 9122.
- In this paper, we adopt the ligand abbreviations [ $\text{PhBP}^{\text{Bu}_2}(\text{pz})$ ] and [ $\text{PhBP}^{\text{Bu}_2}(\text{pz}^{\text{Me}_2})$ ] to refer to a parent pyrazole and a 3,5-dimethyl-substituted derivative, respectively. [ $\text{PhBP}^{\text{Bu}_2}(\text{pz}')$ ] is a general notation to represent any pyrazole derivative.
- (a) Sur, S. K. *J. Magn. Reson.* **1989**, *82*, 169. (b) Evans, D. F. *J. Chem. Soc.* **1959**, 2003.

JA0604358